Quantum mechanical *ab initio* calculations of the Raman scattering from psoralens

2006 J. Phys.: Condens. Matter 18 8325

(http://iopscience.iop.org/0953-8984/18/35/017)

INSTITUTE OF PHYSICS PUBLISHING JOURNAL OF PHYSICS: CONDENSED MATTER

J. Phys.: Condens. Matter **18** (2006) 8325–8336 doi:10.1088/0953-8984/18/35/017

Quantum mechanical *ab initio* calculations of the Raman scattering from psoralens

E M Bezerra[1], M Z S Flores[1], E W S Caetano[1], V N Freire[1], V Lemos[1], B S Cavada[2] and J L de Lima Filho[3]

[1] Departamento de Física, Universidade Federal do Ceará, Centro de Ciências, Caixa Postal 6030, Campus do Pici, 60455-670 Fortaleza, Ceará, Brazil
[2] Departamento de Bioquímica, Laboratório de Bioquímica Molecular, Universidade Federal do Ceará, 60455-670 Fortaleza, Ceará, Brazil
[3] Laboratório de Imunopatologia Keizo Azami, Cidade Universitária, Universidade Federal de Pernambuco, 50670-901 Recife, Pernambuco, Brazil

E-mail: volia@fisica.ufc.br

Received 10 April 2006, in final form 20 June 2006
Published 18 August 2006
Online at stacks.iop.org/JPhysCM/18/8325

Abstract

Calculations of Raman spectra were performed in the case of four furanocoumarins: psoralen, bergapten, xanthotoxin, and isopimpinellin. The Raman bands were assigned by using the results for wavevectors also obtained through these calculations. It is shown that an easy distinction between the four compounds can be obtained by the analysis of the higher wavenumber region of the spectrum where the stretching modes of atoms pertaining to the radicals appear. The use of the other spectral regions is possible for this task, but at the expense of some additional reasoning.

1. Introduction

Linear furanocoumarins, including psoralen and its modifications (xanthotoxin, bergapten, and isopimpinellin), are compounds with strong photobiological phototherapeutic activities [1–3]. In the past they were known as a powerful tool in studying the nucleic acid, DNA, structure and function [4]. Recently, they have been proposed to play an important role in pathogen reduction for the safe storage of blood supply [5, 6]. By covalently modifying DNA, psoralens act as a photosensitizer to affect cell differentiation through interaction with cell surface membranes [7]. Psoralen chemical synthesis being rather expensive, its extraction from natural sources is the usual route. The main sources are tropical plants from the rutaceae family, such as: *R. angustifolia*, with dry weight of 7.8 mg g^{-1} psoralen, 7.2 mg g^{-1} xanthotoxin, 0.3 mg g^{-1} isopimpinellin, and 1.7 mg g^{-1} bergapten; *R. chalepensis*, with dry weight of 1.1 mg g^{-1} psoralen, 0.1 mg g^{-1} xanthotoxin, 0.1 mg g^{-1} isopimpinellin, and 2.6 mg g^{-1} bergapten; *R. graveolens* (Bergamote lime), with dry weight of 1.3 mg g^{-1} psoralen, 1.0 mg g^{-1} xanthotoxin, 0.1 mg g^{-1} isopimpinellin, and 1.6 mg g^{-1} bergapten;

and *R. montana* (Rue), with dry weight of 1.4 mg g^{-1} psoralen, 4.1 mg g^{-1} xanthotoxin, 0.7 mg g^{-1} isopimpinellin, and 1.1 mg g^{-1} bergapten [8]. Other families are known to produce the same compounds but the *Ruta* species contains higher concentrations of furanocoumarins [9]. The bergapten and xanthotoxin compounds are often referred to, alternatively, as 5-methoxypsoralen (5-MOP) and 8-methoxypsoralen (8-MOP), respectively, based on their structural arrangement. Among these compounds, xanthotoxin (8-MOP) is the most used drug, although it competes well with bergapten (5-MOP) in dermatological applications. This latter was found to be better tolerated and to generate fewer side effects than 8-MOP [10]. However, interesting pharmacological applications of 5-MOP were found due to its selective action as an axolemmal potassium blocker. This action is required in a drug for the symptomatic treatment of demyelinating diseases, as in multiple sclerosis [11]. Although all psoralens have similar chemical bondings their biological functions differ considerably. Therefore, it is desirable to clearly identify them, aiming to isolate the structures, for instance by using physical methods.

Raman scattering, among other techniques, is highly appropriate for the identification of psoralen and its modifications due to its great sensitivity to structural arrangements. In order to perform assignments of the experimental modes properly, calculations of Raman spectra associating the detailed vibrational motions to atomic displacements in the molecules are called for. Raman analysis of composites that show pharmacological activity is a promising new tool for their characterization, since it offers some advantages such as the identification of raw materials, quantitative determination of active substances in different formulations, and polymorphic screening support. Vankeirsbilck *et al* [12] pointed out potential applications of Raman spectroscopy in pharmaceutical analysis, weighting the advantages and disadvantages of this technique when applied to drug molecules. It is known that Raman, rather than infrared, spectroscopy is more useful for identifying different crystalline polymorphic forms and molecular conformers, while near-infrared spectroscopy is better suited for detecting similar carbohydrate species and varying hydration states. The ability to theoretically predict physical properties in order to differentiate and/or explain molecular activity (i.e. different conformers and/or slightly different structures for molecules) is receiving attention from industry due to the cost reduction obtained with this strategy by avoiding the unnecessary use of expensive reagents and techniques. In this work we have simulated the Raman spectra of four psoralens (psoralen, bergapten, xanthotoxin, and isopimpinellin) using a first principles Hartree–Fock approach. Theoretical calculations allowed us to find distinctive features in the Raman spectra of psoralen molecules. The vibrational motions involving distinct functional groups of each molecular structure are particularly helpful in achieving such characterization.

2. Method of calculation

The use of digital computers as a tool for molecular simulation has become common. Thanks to the development of first principles methods, especially the density functional theory (DFT) approach, it has been possible to perform molecular geometry optimizations to minimize total energy, determining distances between atoms and angles between bonds, as well as the evaluation of electronic, vibrational and optical properties of systems containing hundreds of electrons and nuclei. Frequencies and intensities of infrared and Raman active modes can be predicted, and are valuable for spectroscopic studies, for instance, to perform dependable assignments by superimposing the calculated spectra of various molecular conformations in the gaseous phase. In particular, the use of *ab initio* techniques to describe the Raman spectrum of molecules is backed up by a massive number of papers published in the literature. Just to cite a few recent works in the field of organic molecules, the article by Hoffmann *et al* [13] reports the

measured frequencies of the fundamental vibrations of anisole in the S-1 state and compares these experimental results with theoretical *ab initio* predictions. Osuna *et al* [14] described the characterization of novel oligothienoacenes with potential applications in the field of organic electronics. Conjugational properties of these materials were investigated using FT-Raman spectroscopy supplemented by DFT and time-dependent DFT (TDDFT) quantum chemical calculations at the B3LYP/6-31G** level, to obtain information concerning the minimum-energy conformation and vibrational normal modes related to the main Raman features. Palafox *et al* [15] calculated the geometry, vibrational wavenumbers, infrared and Raman spectra for the 3-aminobenzonitrile molecule using *ab initio* methods to compare with experimental results, obtaining a very low discrepancy. Characterization of some biomedical compounds with antibiotic, cardiovascular and antimycobacterial activity was performed by Cozar *et al* [16] by using Raman spectroscopy and quantum *ab initio* tools with experimental vibrational bands of Raman spectra confidently assigned on the basis of computational results.

Here, quantum chemical *ab initio* calculations within the restricted Hartree–Fock approximation were performed in two steps: (i) geometry optimization and (ii) vibrational analysis using Gaussian 03 [17]. A 6-31 + G(d) basis set was adopted in both steps, and geometry optimization was considered to be achieved when the rms force acting on all atoms was smaller than 0.3 mHa Å^{-1}. An energy threshold of 10^{-6} Ha was adopted for the self-consistent field (SCF) convergence. All molecules were simulated using the vacuum as dielectric environment (solvation would contribute, at most, a shift of peaks in the Raman spectra). After the molecular geometry was minimized, which correspond to a minimum for the energy, the molecular polarizability tensor was obtained by evaluating the real part of the linear response function [18, 19]:

$$\alpha_{ij}(\omega_0) = \sum_{l>0} \left(\frac{\langle 0|\, \mu^i \,|l\rangle \,\langle l|\, \mu^j \,|0\rangle}{\omega_0 - \omega_l} - \frac{\langle 0|\, \mu^j \,|l\rangle \,\langle l|\, \mu^i \,|0\rangle}{\omega_0 + \omega_l} \right). \tag{1}$$

According to Placzek's polarizability theory [20], the Stokes–Raman differential cross section corresponding to the kth vibrational normal mode, measured perpendicularly to the propagation direction of the incident radiation for a gaseous molecular phase, is given by [21]

$$\perp \left(\frac{\mathrm{d}\sigma}{\mathrm{d}\Omega} \right)_k^n (\pi/2) = \frac{\hbar(\omega_0 - \omega_k)^4}{2c\omega_k} \frac{\left[45\left(\alpha'\right)_k^2 + 7\left(\beta'\right)_k^2 \right]}{45}, \tag{2}$$

where α' and β' are, respectively, the mean polarizability and anisotropy. The $\perp$ symbol denotes that the radiation is linearly polarized, its incidence direction being perpendicular to the scattering plane (which is defined as the plane containing both the incident ray and the observation line). The n index informs that the scattered radiation is measured without polarizers. ω_0 and ω_k correspond, respectively, to the wavenumber associated to the excitation and the kth normal mode of vibration. The mean polarizability α' is obtained through

$$\left(\alpha'\right)_k = \frac{1}{3}\mathrm{Tr}\left(\frac{\partial \boldsymbol{\alpha}}{\partial q_k} \right). \tag{3}$$

Here, $\partial\boldsymbol{\alpha}/\partial q_k$ is the derivative of the polarizability tensor $\boldsymbol{\alpha}$ with respect to the normal coordinate q_k; Tr is the trace of the corresponding tensor. The anisotropy β' is given by

$$\left(\beta'\right)_k = \frac{1}{4} \left\{ \sum_{i,j} \left(\frac{\partial[\alpha_{ii} - \alpha_{jj}]}{\partial q_k} \right)^2 + 6 \sum_{\substack{i,j \\ i \neq j}} \left(\frac{\partial \alpha_{ij}}{\partial q_k} \right)^2 \right\}. \tag{4}$$

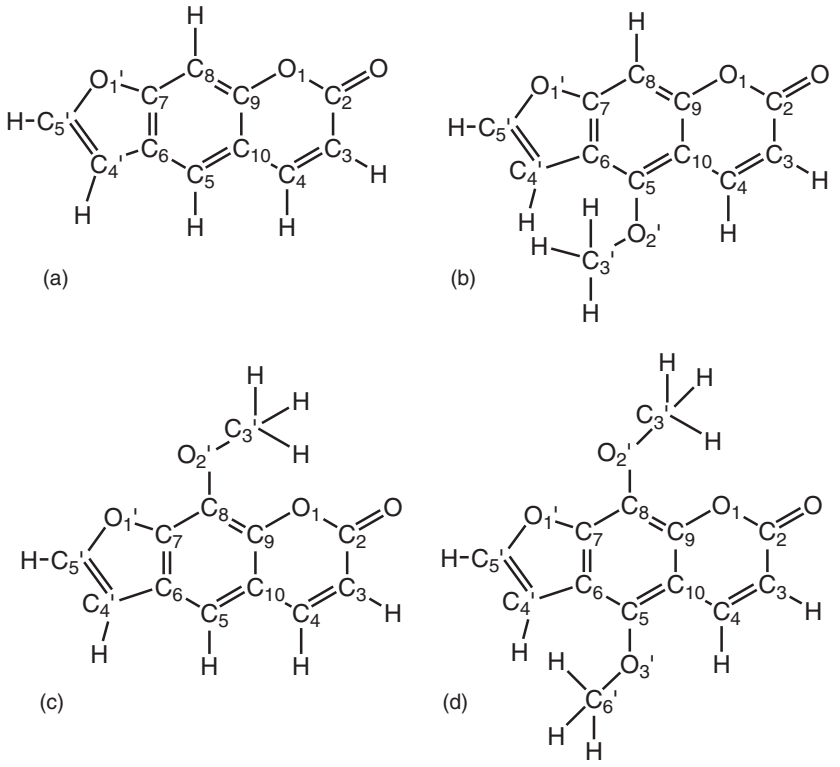

Figure 1. Structure of (a) psoralen, (b) bergapten, (c) xanthotoxin, and (d) isopimpinellin.

On the other hand, derivatives with respect to the normal coordinates q_k are related to the nuclear coordinates x_l through

$$\frac{\partial \alpha_{ij}}{\partial q_k} = \sum_{l=1}^{3N} \frac{\partial \alpha_{ij}}{\partial x_l} \frac{s_{lk}}{\sqrt{m_l}}, \tag{5}$$

where s_{lk} is the lth component of the kth normal mode eigenvector and m_l is the mass of the corresponding atom. Polarizabilities used in these equations should be divided by $4\pi\epsilon_0$. Derivatives are always calculated at the optimized geometry and using the method proposed by Frisch *et al* [22] and Yamaguchi *et al* [23]. The Raman spectrum was calculated for all the studied molecules using the same procedure. As an extra convergence criterion, the calculated normal modes of vibration were analysed in order to ensure that all wavenumbers were positive (if there were negative wavenumbers after achieving the convergence criterion, the computed geometry would represent a saddle point in the configuration space and not a suitable molecular geometry).

3. Results and discussion

The basic structure of the psoralen molecule is represented in figure 1(a). Figures 1(b)–(d) give the structures of the compounds bergapten, xanthotoxin, and isopimpinellin, respectively. The basic structure is formed with three rings, namely, furan-, benzene-, and pyron-rings. The

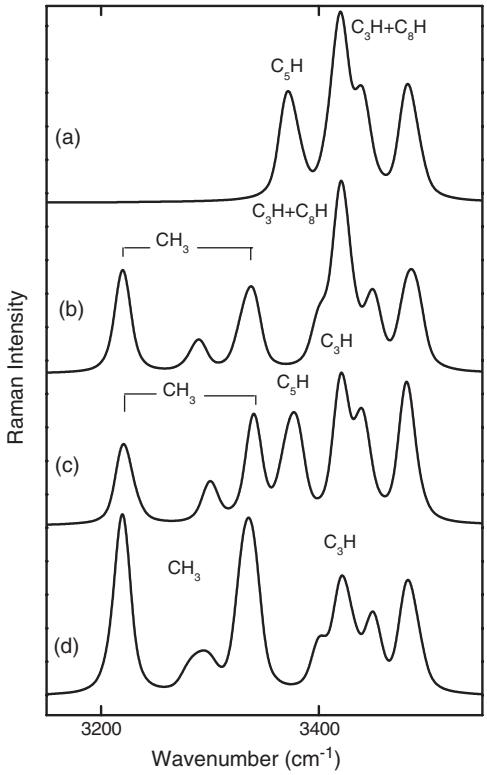

Figure 2. Raman spectrum in the range [3150, 3350] cm^{-1} from (a) psoralen, (b) bergapten, (c) xanthotoxin, and (d) isopimpinellin.

atomic numbering follows the convention with the benzene- and pyron-rings labelled with arabic numbers and the primed numbers labelling atoms out of these rings. In particular, those carbon atoms in the $–OCH_3$ radicals are numbered C'_3 and C'_6. The bergapten structure, or 5-methoxypsoralen (5-MOP), has the hydrogen bonded to carbon 5 in psoralen substituted by a $–OCH_3$ radical. In xanthotoxin the same type of substitution occurs but at carbon 8, and it is also known as 8-methoxypsoralen (8-MOP). In isopimpinellin, two such substitutions occur at both carbon atoms, and the compound is named as 5,8-dimethoxypsoralen (5,8-MOP), accordingly.

The two hexagonal rings in psoralen comprise 15 atoms, and the pentagonal ring adds 5 more atoms, making a total of 20 atoms in the molecule. Group theory attributes 60 degrees of freedom, among which 3 count for the translational motions giving rise to the acoustic phonons and 3 for the rotational degrees. The remaining 54 degrees of freedom stand for the vibrational motions in the molecule. Psoralen belongs to the triclinic space group $P1$, the lowest symmetry group. Due to the lack of symmetry, all 54 modes comes from the totally symmetric one-dimensional representation A, and are predicted to be, simultaneously, Raman and infrared active. Similarly, 66 vibrational modes are expected for either 5-MOP or 8-MOP and 78 for isopimpinellin. The results for all psoralens are displayed in figures 2–4, separated into spectral regions for the sake of clarity. Three spectral regions were selected due to the distinctive features observed for each of the four compounds in the spectra. They will be referred to as high-, medium- and low-wavenumber regions, for the ranges [3150–3550] cm^{-1},

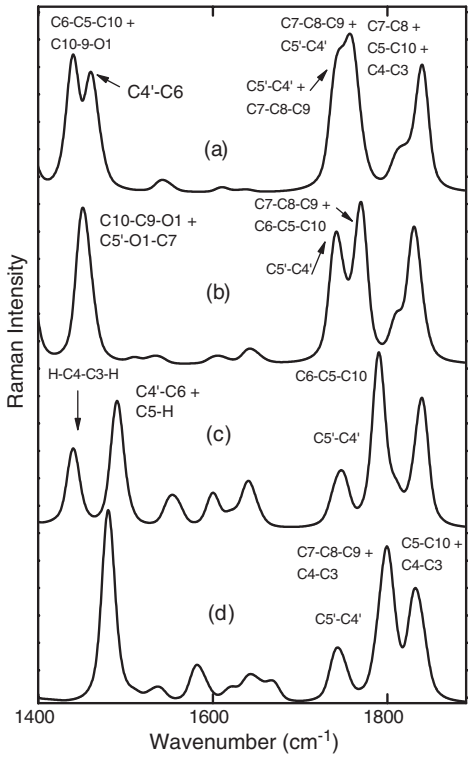

Figure 3. Raman spectrum in the range [1400, 1890] cm^{-1} from (a) psoralen, (b) bergapten, (c) xanthotoxin, and (d) isopimpinellin.

[1400–1880] cm^{-1}, and [350–750] cm^{-1}, respectively. The overall results, including the type of atomic motion assigned to the modes, are listed in the respective tables.

In the discussion following we focus first on the highest wavenumber region because it contains the most important clues for distinguishing the four psoralens. Figure 2 shows the high-frequency region of the spectra in the sequence: (a) psoralen; (b) bergapten (5-MOP); (c) xanthotoxin (8-MOP); (d) isopimpinellin (5,8-MOP). The three lower wavenumber peaks, marked CH_3 in the figure, are not present in the spectrum of psoralen. In curve (b) they appear at 3220, 3288, and 3336 cm^{-1}, and correspond to C3′H stretching vibrations in the radical of the 5-MOP structure, and are listed in table 1, accordingly. The figure shows, in curve (c), that this type of motion in xanthotoxin gives rise to peaks extremely close in position, at 3222, 3300, and 3340 cm^{-1}. In 5,8-MOP there are two radicals, C3′H, and C6′H; the stretching type vibrations give rise to unresolved pairs in figure 2(d) calculated to peak at [3217, 3220] cm^{-1}, [3284, 3296] cm^{-1}, and [3333, 3337] cm^{-1}. Because the wavenumbers are accidentally quasi-degenerated for the motions in the two radicals, the bands in the spectra are stronger than those for 5- and 8-MOP. Next in position, two bands are distinguished, appearing selectively in the spectra for psoralen and xanthotoxin, curves (a) and (c) in figure 2. They are due to the unresolved pair [3369, 3374] cm^{-1} in the first, and [3371, 3376] cm^{-1} in 8-MOP. Table 1 lists a series of C–H anti-symmetric stretchings involving the carbon atoms C_5, C_4, and C_3, corresponding to these positions. However, these bands, marked C_5H in the figure, are not seen in the spectra for the other two compounds, bergapten and isopimpinellin. These strong

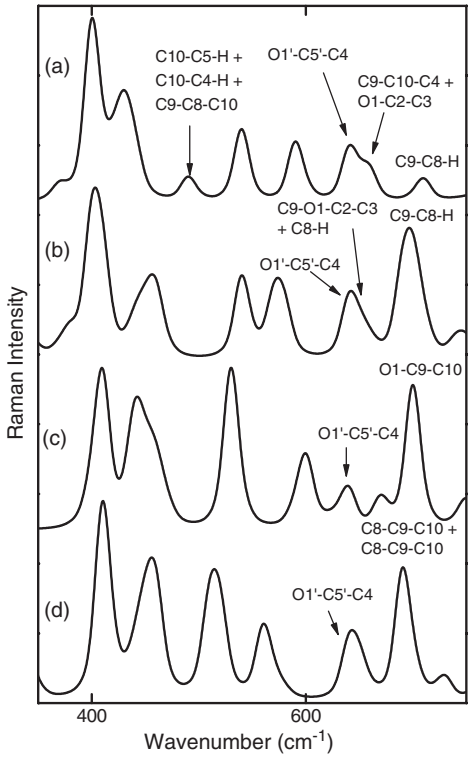

Figure 4. Raman spectrum in the range [350, 750] cm^{-1} from (a) psoralen, (b) bergapten, (c) xanthotoxin, and (d) isopimpinellin.

structures occurring in psoralen and 8-MOP spectra, exclusively, have a particular reason: the dominant type of motion is the C_5–H anti-symmetric stretching, which is possible in both compounds but impossible in 5-MOP or 5,8-MOP.

We next analyse strong features appearing in the psoralen and bergapten spectra due to the unresolved pairs of peaks [3415, 3423] cm^{-1} and [3419, 3423] cm^{-1}, respectively. These lines, labelled $C_3H + C_8H$ in figure 2, correspond to the anti-symmetric stretching C_8–H and C_3–H, according to our assignments as listed in table 1. The C_8–H anti-symmetric stretching does not contribute to the 8-MOP or 5,8-MOP spectra due to C_8 bonds with radicals. Therefore, the peaks at 3421 cm^{-1}, 3423 cm^{-1} in the 8-MOP and 5,8-MOP spectra are mainly related to the C_3H stretching. A distinction between the latter can be noted in figure 2: in curve (d), this peak is preceded by a shoulder related to a C_4H stretching motion. This shoulder appears also in the case of 5-MOP, as can be checked in the assignment of the 3401 cm^{-1} peak listed in table 1. The remaining structures, corresponding to the CH-stretching type of motion in the furan-ring, are practically the same, as expected, since this ring is equal in all structures. The remaining structures in the spectra of figure 2 are due to vibrations involving carbon atoms of the furan-ring. As the furan-ring is common to all four compounds, the related motions should not generate distinguished features in the spectra. Figure 2 shows that this is, actually, the case for the highest wavenumber peaks present in the four spectra.

It should be reinforced that the analysis of the 3100–3600 cm^{-1} region of the spectrum alone allows for a distinction between the four compounds to be made. Psoralen is exclusive

Table 1. Calculated wavenumbers in units of cm^{-1}, and corresponding vibration assignment. The asterisk is for the stronger amplitudes and the letters R, W, T, Sc, A, and S, stand for rocking, wagging, twisting, scissoring, anti-symmetric stretching, and symmetric stretching, respectively.

Psoralen		Bergapten (5-MOP)		Xanthotoxin (8-MOP)		Isopimpinellin (5,8-MOP)	
ω	Assignment	ω	Assignment	ω	Assignment	ω	Assignment
						3217	*S C6′H
							S C3′H
		3220	*S C3′H	3222	*S C3′H	3220	*S C6′H
							S C3′H
		3288	A C3′H			3284	A C6′H
				3300	A C3′H	3296	A C3′H
						3333	A C6′H
		3336	A C3′H	3340	A C3′H	3337	A C3′H
3369	*A C5–H			3371	*A C5–H		
	*A C4–H				*A C4–H		
	A C3–H				A C3–H		
3374	*A C5–H			3376	*A C5–H		
	*A C4–H				*A C4–H		
	A C3–H				A C3–H		
		3401	*A C4–H			3402	*A C4–H
			A C3–H				A C3–H
3415	*A C8–H	3419	*A C8–H				
3423	*A C3–H	3423	*A C3–H	3421	*A C3–H	3423	*A C3–H
	A C4–H		A C4–H		A C4–H		A C4–H
3441	*A C4′–H	3449	*A C4′–H	3441	*A C4′–H	3449	*A C4′–H
	A C5′–H		A C5′–H		A C5′–H		A C5′–H
3483	A C4′–H	3485	A C4′–H	3482	A C4′–H	3484	A C4′–H
	*A C5′–H		*A C5′–H		*A C5′–H		*A C5′–H

because there is no CH_3 stretching related peak in its spectrum. Among the radical contained compounds, just the xanthotoxin Raman spectrum has a C_5H band. The remaining 5-MOP and 5,8-MOP can be distinguished because the C_3H stretching related vibrations generate bands twice as strong in the latter. Although the distinction is accomplished by performing just a partial analysis, a detailed discussion should be performed in order to have a more complete picture. In this sense, we include the lower wavenumber spectral regions as follows.

The medium wavenumber region spectra in figure 3 are displayed for (a) psoralen, (b) 5-MOP, (c) 8-MOP, and (d) 5,8-MOP, showing distinguished features around 1450 cm^{-1}. For psoralen, two peaks appear at 1439 and 1463 cm^{-1}, respectively. Two peaks appear also in the spectrum for 8-MOP, at 1441 and 1491 cm^{-1}, respectively. In the case of 5-MOP and 5,8-MOP, just one peak is present at the corresponding spectrum, positioned at 1453 and 1481 cm^{-1}, respectively. Therefore, inspection of the Raman spectra in this region can help in the task of identification. The vibrations are complex combinations of the several types of motion (see table 2), making it difficult to perform an easy labelling. However, it can be seen that they involve atoms belonging to the rings, but not atoms from the radicals. The peak appearing at about 1440 cm^{-1} in psoralen and xanthotoxin, for instance, has very similar contributions of a symmetrical stretching among carbon atoms (S C6–C5–C10), three anti-symmetrical stretching motions (A C10–C9–O1, A O1′–C7, A C6–C4′) and two wagging motions (W H–C4–C3–H, W C4′–H or W C5′–H). The psoralen peak is more intense than the related xanthotoxin peak, probably due to the stretching motions being stronger in the first compound. We label the peaks in figure 3 according to the assignments listed in table 2, selecting only the strongest

Table 2. Calculated wavenumbers in units of cm^{-1}, and corresponding vibration assignment. The asterisk is for the stronger amplitudes and the letters R, W, T, Sc, A, and S, stand for rocking, wagging, twisting, scissoring, anti-symmetric stretching, and symmetric stretching, respectively.

Psoralen		Bergapten (5-MOP)		Xanthotoxin (8-MOP)		Isopimpinellin (5,8-MOP)	
ω	Assignment	ω	Assignment	ω	Assignment	ω	Assignment
1439	*S C6–C5–C10 *A C10–C9–O1 A O1′–C7 A C6–C4′ W H–C4–C3–H A C10–C4 W C4′–H			1441	S C6–C5–C10 A C10–C9–O1 A O1′–C7 A C6–C4′ *W H–C4–C3–H W C5′–H		
1463	A C10–C9–O1 S C5′–O1′ *S C4′–C6 W C5′–H S C7–C8	1453	*A C10–C9–O1 *A C5′–O1′–C7 A C4′–C6 W C5′–H W H–C4–C3–H				
				1491	*S C4′–C6 W H–C4–C3–H Sc C6–C5–C10 *W C5–H A C4′–C6–C7 S C5′–O1′	1481	A C4′–C6 W H–C4–C3–H A O1–C5–C10 A O1′–C7–C6 S C8–O2′
1744	*S C5′–C4′ A C6–C5–C10 *S C7–C8–C9 W C8–H, W C5–H	1743	*S C5′–C4′ A C6–C5–C10 S C7–C8–C9 A C4–C3 W C8–H	1746	*S C5′–C4′ A C6–C5–C10 S C7–C8–C9 A C4–C3 W C5–H	1744	*S C5′–C4′ A C6–C5–C10 S C7–C8–C9 A C4–C3
1762	*S C7–C8–C9 *S C6–C5–C10 A C5′–C4′ A C4–C3	1768	*S C7–C8–C9 *S C6–C5–C10 A C5′–C4′ S C4–C3 Sc C3′H				
				1790	S C7–C8–C9 *S C6–C5–C10 A C5′–C4′ A C4–C3 Sc C3′–H	1797	*S C7–C8–C9 A C6–C5–C10 S C5′–C4′ *S C4–C3 Sc C3′–H
				1807	*A C6–C5 *S C3–C4 *A C7–C8–C9 W C5–H	1805	*S C6–C5 *S C8–C9 A C4–C10 A C7–O1′ W C4′–H Sc C3′–H
1815	*S C5–C6 *A C7–C8–C9 S C4–C3 A C7–O1′ W C5–H W C4′–H W C4–H	1811	*S C5–C6 *A C7–C8–C9 S C4–C3 A C7–O1′ W C5–H W C4′–H Sc C3′–H				
1838	*S C7–C8 *S C5–C10 *S C4–C3 A C9–O1 W C5–H, W C8–H	1832	*S C7–C8 *S C5–C10 *S C4–C3 A C9–O1 W C8–H	1838	*S C7–C8 *S C5–C10 *S C4–C3 A C9–O1 W C5–H Sc C3′–H	1834	S C7–C8 *S C5–C10 *S C4–C3 A C9–O1 Sc C3′–H

components for the display. Also, in curves (b) and (c) of figure 3 the last peak was not labelled because its identification is the same as in (a). The features around 1800 cm^{-1} in figure 3 constitute another key for distinction of the compounds. The reason is the following: the feature at about 1750 cm^{-1} is an unresolved pair of peaks in psoralen, a well resolved pair in bergapten, and single peaks in the remaining compounds. For the distinction between 8- and 5,8-MOP, the separation between the two bands following the single peak has to be analysed. The smaller separation occurs in the spectrum for 5,8-MOP. We describe next the wavevectors corresponding to these features aiming at a more complete assignment, by using the results listed in table 2. In the psoralen spectrum, the strong unresolved structure corresponds to the positions listed as 1744 and 1762 cm^{-1} in table 2. For 5-MOP the well resolved features peak at 1743 and 1768 cm^{-1}, as listed in the table. The first peak (at about 1744 cm^{-1}) has a strong contribution from a stretching C5′–C4′ in all four compounds. The second component, which is unresolved in psoralen but well resolved in bergapten, has strong contributions from symmetric stretching motions of carbon atoms from the rings. In the other two compounds this type of motion generates the 1790 and 1797 cm^{-1} peaks. Stretching among carbon atoms causes the appearance of the peak at about 1835 cm^{-1} for all psoralens and the preceding shoulders in the first two compounds.

Finally, we analyse the low wavenumber region chosen as the [350–750] cm^{-1} range. The Raman spectra are shown in figure 4 following the usual order for the display. This region comprises rocking, scissoring, twisting and wagging motions, as detailed in table 3. The vibration amplitudes are smaller than those of stretching motions, and the peak intensities in this region are about one order of magnitude weaker. The first two strong features comprise a single mode peaking between 401 and 440 cm^{-1}, followed by an accidentally doubly degenerate mode. These features being quite similar in all compounds, their use should not be attempted as a distinguishing key. A not so strong peak, appearing exclusively for psoralen at 491 cm^{-1}, could be used as a selective tool. It corresponds to the combined twisting motions C10–C5–H, C10–C4–H, and C9–C8–C10, according to the assignments listed in table 3. Therefore, this peak is labelled in figure 4, even though the motions are not strong. The following pair of peaks appearing between 515 and 598 cm^{-1} are distinguished only through small differences in relative intensities and small separations. Because of these similarities they should not be used to identify any of the four compounds. The end of region features are interesting for this task due to sizable differences. The last peak, positioned at about 700 cm^{-1}, is weak only in the psoralen spectrum. It is a wide-band only in the bergapten spectrum, due to an accidental degeneracy between the 692 and 703 cm^{-1} modes. In the remaining two compounds, the preceding features are two well resolved peaks appearing at 637 and 670 cm^{-1} in the xanthotoxin spectrum, against an unresolved doublet in the isopimpinellin spectrum. Therefore, these features are also reasonable tools in distinguishing between the psoralens. In figure 4 these structures are labelled according to the corresponding wavevector as described in table 3. It should be reinforced once again that the best tools, however, are found in the higher wavenumber region.

4. Conclusions

Raman spectra were calculated for psoralen, bergapten, xanthotoxin, and isopimpinellin. The calculated wavevectors allowed for the assignment to be made for all Raman active modes predicted. The results are helpful in distinguishing between the four compounds. This task is readily performed by the analysis of the higher wavenumber region of the spectrum. This is the region were stretching modes of atoms pertaining to the radicals appear. The remaining regions

Table 3. Calculated wavenumbers in units of cm^{-1}, and corresponding vibration assignment. The asterisk is for the stronger amplitudes and the letters R, W, T, Sc, A, and S, stand for rocking, wagging, twisting, scissoring, anti-symmetric stretching, and symmetric stretching, respectively.

Psoralen		Bergapten (5-MOP)		Xanthotoxin (8-MOP)		Isopimpinellin (5,8-MOP)	
ω	Assignment	ω	Assignment	ω	Assignment	ω	Assignment
440	T C5–C10–C4 T C4′–C5′–H	446	Sc O3′–C5–C10 Sc C2–C3–C4 W O1–C2–C3 W C7–C8–H	446	*R C10–C4–C3 T O1′–C5′–H R C8–C9–O1	446	*R C10–C4–C3 T O1′–C5′–H R C8–C9–O1
		461	*R C10–C4–C3 T C9–C8–H W C4′–H Sc C8–O2′–C3′H	463	R C8–C9–01 R C10–C4–C3 T C10–C5–H	459	W C6′H W O1–C2–O Sc C10–C4–C3
491	T C10–C5–H T C10–C4–H T C9–C8–C10						
						515	W C8–O2′–C3′H W C5–O3′–C6′H T C1O–C4–H W C3–H
540	Sc H–C3–C2–H W C8–H Sc C9–C10–C5 W C4–H	541	*Sc H–C3–C2–O W C8–H Sc C9–C10–C5 W C4–H Sc C9–O1–C2	531	W C3′H T C10–C5–H W C4–H Sc H–C3–C2–O		
						562	Sc C7–C6–C5 R O3′–C6′H R O2′–C3′H
		575	Sc C7–C6–C5 R O3–C3′H T C7–C8–C9			576	*T C10–C4–H Sc C8–O2′–C3′H W C3–H R C7–C8–C9
592	Sc C5–C6–C4′–H W C9–C8–C2 Sc C4–C3–C2			598	R O3′–C3′H T C10–C5–H W H–C4–C3–H		
643	*R O1′–C5′–C4′ T C7–C8–H T C6–C5–H	641	*R O1′–C5′–C4′	637	*R O1′–C5′–C4′ T C10–C4–H W C3–H	641	*R O1′–C5′–C4′
658	*W C9–C10–C4 *W O1–C2–C3 Sc C7–C8–C9	654	*Sc C9–O1–C2–C3 W C5′–C4′–H *W C8–H			652	R C8–O2′–C3′ R C5–O3′–C6′ Sc C4′–C6–C5 W O1′–C5′–H
				670	R C5′–C4′–C6′ T C6–C5–H T C10–C4–H T C2–C30H W C8–O2′–C3′		
		692	*T C9–C8–H T C10–C4–H T C3–C4–H Sc O1–C2–O			692	Sc O1–C2–O S C8–C9–C10
708	*T C9–C8–H T C10–C4–H T C2–C3–H	703	*T C9–C8–H T C10–C3–H W O2′–C3′H	700	T C10–C5–H *Sc O1–C9–C10 T C4–C3–H W O2′–C3′H		

of the spectrum are also suitable, but their analyses are complicated due to the combination of several different types of motion for each wavenumber.

Acknowledgments

The authors are indebted to Professor S Canuto for the use of the Gaussian software. This work was stimulated by the life work of Professor Dr F J Abreu Matos on biological properties of Brazilian medicinal plants developed at the Organic Chemistry Department, Universidade Federal do Ceará. Financial support was received from Conselho Nacional de Desenvolvimento Científico e Tecnológico, CNPq, and Fundação Cearense de Apoio ao Desenvolvimento Científico e Tecnológico, FUNCAP. VNF and BSC are senior researchers from CNPq and acknowledge the grant for Rede NanoBioestruturas 555183/2005-0. VL acknowledges grant CNPq–DCR 303818/04-5. MZSF is sponsored by a graduate fellowship from CNPq.

References

[1] Yurkow E and Laskin J 1990 *Toxicology* **65** 33
[2] Zarebska Z, Waszkowska E, Caffieri S and Dall'Acqua F 1990 *Farmaco* **55** 515
[3] Peters B, Weissman F G and Gill M A 1990 *Am. J. Health-Syst. Pharm.* **57** 645
[4] Cimino G, Dna H G, Isaacs S T and Hearst J 1985 *Annu. Rev. Biochem.* **54** 1151
[5] Margolis Nunno H *et al* 1997 *Transfusion* **37** 889
[6] Wu Y and Snyder E 2003 *Blood Rev.* **17** 111
[7] Lanskin J 1994 *Food Chem. Toxicol.* **32** 119
[8] Bourgaud F, Allard N, Guckert A and Forlot P 1989 *Natural Sources of Furocoumarins* (Paris: Libbey Eurotext) pp 219–30
[9] Milesi S, Massot B, Gontier E, Bourgaud F and Guckert A 2001 *Plant Sci.* **161** 189
[10] Berg M and Ros A 1993 *Life Sci.* **53** 355
[11] Bohuslavizki K *et al* 1994 *Eur. J. Pharmacol.* **46** 375
[12] Vankeirsbilck T *et al* 2002 *Trends Anal. Chem.* **21** 869
[13] Hoffmann L J H, Marquardt S, Gemechu A S and Baumgartel H 2006 *Phys. Chem. Chem. Phys.* **8** 2360
[14] Osuna R M, Zhang X N, Matzger A J, Hernandez V and Navarrete J T L 2006 *J. Phys. Chem.* A **110** 5058
[15] Palafox M A, Rastogi V K, Mittal L, Kiefer W and Mital H P 2006 *Int. J. Quantum Chem.* **106** 1885
[16] Cozar O, Chris V, David L and Baias M 2006 *J. Optoelectron. Adv. Mater.* **8** 164
[17] Frisch M *et al* 2003 *Gaussian 03,* Revision A.1 (Pittsburgh, PA: Gaussian)
[18] Olsen J and Jorgensen P 1985 *J. Chem. Phys.* **82** 3235
[19] Vidal L N and Vazquez P A M 2003 *Quim. Nova* **26** 507
[20] Placzek G 1959 The Rayleigh and Raman Scattering United States Atomic Energy Commission: Lawrence Radiation Laboratory, University of California, Livermore, California, UCRL Translation n. 526 (L), Physics
[21] Long D A 2002 *The Raman Effect, A Unified Treatment of the Theory of Raman Scattering by Molecules* (England: Wiley)
[22] Frisch M J, Yamaguchi Y, Gaw J F, Schaefer H F and Binkley J S 1986 *J. Chem. Phys.* **84** 531
[23] Yamaguchi Y, Frisch M, Gaw J, Schaeffer H F and Binkley J S 1986 *J. Chem. Phys.* **84** 2262